Modeling heat and mass transfer within a wall built of BTC

Abstract

Numerical modelling of coupled heat and mass transfer within a BTC wall is presented.Drawing on the work of Luikov, a mathematical model governing heat and mass transfer was established.Temperature and moisture content were chosen as potential transfer drivers.The problem was tackled using a numerical approach (finite element method).Implementing the mathematical model in COMSOL enabled us to obtain very convincing results. The results show that the optimum thickness found is 40 cm. Moisture content and temperature have no effect when thickness exceeds 40 cm.

Keywords: Mass transfer, BTC, coupled, Heat transfer, Comsol

Nomenclature: Certain notations, used locally, are no longer mentioned in the list below. They are explained as they appear in the text

Latin characters

$C_{p,a}$: specific heat of dry air (J/kg/K) ;

$C_{p,l}$: specific heat of liquid water (J/kg/K) ;

$C_{p,m}$: specific heatof dry material (J/kg/K) ;

L_v : latent heat of change of state (J/kg)

C_T : total specific heat of the porous material (J/kg/K)

K :hydraulic conductivity (kg/Pa.m.s)

M :molar mass of water (kg/mol)

$\dot{m}$: flux density (kg/m^2.s) ;

n : vector normal to the exchange surface;

$\dot{m}_l$: liquid flux density(kg/m^2.s) ;

$\dot{m}_v$: vapor flux density (kg/m^2.s);

$\dot{m}_T$: mass flux density under temperature gradient (kg/m^2.s);

P_v^{sat} : saturation vapor pressure (Pa) ;

P_c : capillary pressure (Pa);

P_v : partial vapor pressure ;

q : flux de chaleur (W/m^2) ;

R_v : constante de la vapeur d'eau (J/kg.K)

T_{ext} : ambient temperature (K);

T_{int} : wall surface temperature (K);

t : times (s) ;

v :air speed (m/s)

Lettres grecques :

φ_{ext} : outdoor relative humidity (.);

φ_{int} :indoor relative humidity (.);

β : masse transfert coefficient(kg/m^2.s.Pa);

δ_p : vapor permeability of wet material (kg/m.s.Pa);

α : heat transfer coefficient (W/m^2.K).

ρ_v : density of water vapour (kg/m^3) ;

ρ_m : density of matérial (kg/m^3)

ρ_l : densityofwater liquid (kg/m^3)

ω : mass water content (kg/m^3) ;

Ω : moisture storage capacity (kg/m^3.Pa) ;

λ : thermal conductivity of the material (W/m.K).

Indices :

a : air ;

c : capillary ;

ext. :outdoor ;

int. : indoor

l : liquid ;

m : material ;

p : permeability ;

T : temperature ;

v : vapor.

1. Introduction

Global energy consumption is rising steadily in almost all sectors, and particularly in the building industry.According to [Xianwei Liu et al, 2015 (numerical...)] the share of energy demand for buildings in total energy consumption has increased rapidly in recent decades. Energy consumption in buildings is estimated at 35% of total energy consumption [Xiangwei Liu et al, 2015 (determinat...)]. China, one of the world's biggest energy consumers, is sounding the alarm about the crucial issue of energy security [Xianwei Liu et al, 2015 (numerical...)].This consumption could be accelerated in buildings with the improvement in people's living conditions and the need for thermal comfort especially in urban environments (Liu Rong et al, 2018). The need for thermal comfort for building occupants generally involves finding the comfort zone.Some studies have shown that the comfort zone can be achieved by active or passive cooling using bioclimatic building design methods in a dry tropical climate (IEPF, 2008).In Burkina Faso, as in most Sahelian countries, the need for energy for air conditioning is growing steadily.This requirement is estimated at 30,000 MWh/year, corresponding to a financial cost of around 3.4 billion FCFA/year (DGE, 2003).Indeed, the climatic environment in buildings is subject to various internal and external stresses that have an effect on their hygrothermal behavior (Mohamed Sawadogo et al, 2023).Heat and moisture transfer in walls affects the thermal performance of building materials and building energy consumption (Liu Rong et al .2018), (Xianwei Liu et al, 2015) points out that moisture storage in porous building envelopes strongly influences the thermal performance of buildings.Heat transfer through the building envelope therefore remains the main cause of energy consumption (Lamyaa Laou et al., 2023). Indeed, heat loss from the building envelope plays a major role in energy wastage (Sabhas Mishra et al, 2012).Faced with the challenges of energy saving and environmental sustainability, building envelope management could be the ideal solution.To limit these energy costs, research and development work is being carried out on both materials and wall design.Some studies have estimated the transmission load through the exterior wall into the room using a numerical method (Xianwei Liu et al), which neglects the effect of moisture transfer on heat transmission.The study of coupled heat and moisture transfer in porous building materials dates back decades

(Mohamed Sawadogo et al. 2023).There are several theoretical models in the literature that study coupled heat and mass transfer.However, the most widely used and accepted are the Luikov and Philip and De Vries models (Mohamed Sawadogo et al. 2023).In the literature, few studies have been devoted to solving coupled 2D/3D heat and mass transfer problems in the unsteady regime of a building wall based on porous materials.The present work is based on Luikov's model and that of Philip and De Vries implemented in COMSOL Multiphysics.Comsol software uses the finite element method to solve equations.Temperature and humidity are the potential drivers used in our model.In this work we propose a 3D numerical study of coupled heat and moisture transfer in order to understand the spatio-temporal distribution of moisture content and temperature within a wall made of Compressed Earth Brick (CEB).This model is used to simulate temperature and moisture content distributions across the BTC wall.Analysis of the results obtained will enable us to deduce the optimum wall thickness at which insulation is no longer necessary.

2. materials and methods

In this study, we consider a low wall composed of compressed earth bricks (C.E.B.) and cement mortar, whose

thermophysical properties are given in Table 1.The wall dimensions are 90.5 cm x 30 cm x 14 cm. The BTC were stabilized with 8% CPJ 45 cement.Thermophysical properties such as thermal conductivity, thermal diffusivity and specific heat were measured using the KD 2 PRO.Table 1 below shows the values obtained and used in the simulation.

a. Physical models

BTCs are hygroscopic materials [J. Emmanuel Aubert et al. 2013] and also phase-change materials under the influence of a temperature and/or humidity gradient.In this study, we propose a physical model consisting of a wall made of BTC grouted with mortar (1 cm thick) consisting of sand, cement and water (figure 1).The thermophysical properties of BTC are obtained experimentally from the work of (Kabré et al., 2019). Figure 2 shows a photo of the KD 2 PRO used for the measurements.

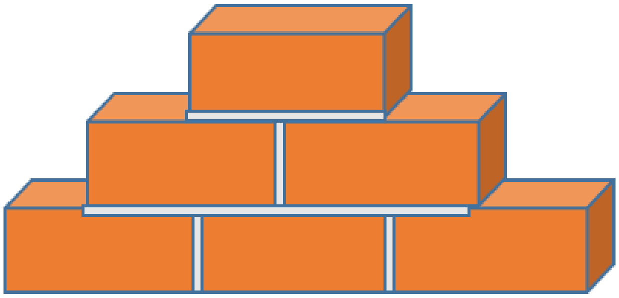

Figure 1: wall model

Figure 2: Photo of KD2 Pro device

b°) Mathematical model of coupled heat and moisture transfer in the wall

In porous materials such as BTC, heat and moisture transfer processes are closely linked. The concepts developed by the pioneers of coupled heat and mass transfer modelling are still relevant today.These different models differ in their choice of the main potential transfer drivers. The present work is based on Luikov's model.The potential transfer drivers selected for this work are temperature and humidity.The mathematical model used in this manuscriptis based on the conservation of energy and mass

For modelling heat and mass transfer through the low wall studied, the governing equations are given by 1 and 2 based on the Luikovmodel:

$$(c_{p,m}\rho_m + c_{p,l}\rho_l)\frac{\partial T}{\partial t} = \nabla\left(-\lambda\nabla T\right) + L_v\nabla(\dot{m}_v) \quad (1)$$

$$\frac{\partial \omega}{\partial t} + \nabla(\dot{m}_l + \dot{m}_v) = 0 \; (2)$$

c) Simplifying assumptions

The model chosen is based on the following assumptions:

- ➢ The porous material is assumed to be homogeneous, isotropic and dimensionally stable,
- ➢ The liquid phase is not taken into account,
- ➢ The properties of the gas phase are taken as those of a perfect gas,
- ➢ The driving forces behind the transfers are the outdoor air temperature T and the outdoor air humidity φ,

- Liquid water does not flow across the contact surface. Any water flowing towards external surfaces is in vapor form.

d) Formulation of the numerical model

The equations governing the transfers involved in our model are based on those proposed by (De Vries 1957) and (Luikov 1975).Taking into account the above assumptions, the development of equations (1) and (2) gives :

$$(c_{p,m}\rho_m + c_{p,l}\rho_l)\left(\frac{\partial T}{\partial t}\right) + \nabla(k_v\nabla\omega + \lambda^*\nabla T) = 0 \quad (3)$$

$$\frac{\partial\omega}{\partial t} + \nabla\left((k_v + k_l)\nabla\omega + (\delta_v + \delta_l)\nabla T\right) = 0 \quad (4)$$

Posing $C_T = C_{p,m}\rho_m + C_{p,l}\rho_l$,

$\beta^\omega = k_v + k_l$ and $\beta^T = \delta_v + \delta_l$

The two equations (3) and (4) can be expressed as follows:

$$\begin{cases} c_T\dfrac{\partial T}{\partial t} + \nabla(k_v\nabla\omega + \lambda^*\nabla T) = 0 \\ \dfrac{\partial\omega}{\partial t} + \nabla(\beta^\omega\nabla\omega + \beta^T\nabla T) = 0 \end{cases} \quad (5)$$

Equation (6) is obtained from equation (5) by changing the parameters.

$$\begin{cases} \dfrac{\partial T}{\partial t} + \nabla(C_{11}\nabla T + C_{12}\nabla\omega) = 0 \\ \dfrac{\partial\omega}{\partial t} + \nabla(C_{21}\nabla T + C_{22}\nabla\omega) = 0 \end{cases} \quad (6)$$

e. Initial and boundary conditions

- **Initial conditions**

The values of temperature and water content initialized at time t_0 are such that:

$$T(x, y, z, t) = T(t = t_0) = T_0 \quad (7)$$

$$\omega(x, y, z, t) = \omega(t = t_0) = \omega_0 \quad (8)$$

t_0 being the instant at which interaction between the wall and the surrounding environment begins.

- **Boundary conditions**

The boundary conditions used for the numerical simulation are:

- the wall being semi-infinite according to(ox) and (oz) the top surfaces(x = L, y = l, z = h)andinferior(x = L, y= l, z = 0)and side faces(x = 0, y = l, z = h) and (x = L, y = 0, z = h)are adiabatic and insulated. The heat and mass flows are then zero, which translates into:

$$\left(\frac{\partial T}{\partial y}\right)_{x=0,z} + \left(\frac{\partial T}{\partial z}\right)_{x=0,y} = 0 \quad (9)$$

$$\left(\frac{\partial T}{\partial y}\right)_{x=L,z} + \left(\frac{\partial T}{\partial z}\right)_{x=L,y} = 0 \quad (10)$$

$$\left(\frac{\partial T}{\partial x}\right)_{y,z=0}+\left(\frac{\partial T}{\partial y}\right)_{x,z=0}=0 \quad \left(\frac{\partial T}{\partial x}\right)_{z,y=0}+\left(\frac{\partial T}{\partial z}\right)_{x,y=0}=0$$ (11)

$$\left(\frac{\partial \omega}{\partial y}\right)_{x=0,z}+\left(\frac{\partial \omega}{\partial z}\right)_{x=0,y}=0$$ (13) (12)

$$\left(\frac{\partial \omega}{\partial y}\right)_{x=L,z}+\left(\frac{\partial \omega}{\partial z}\right)_{x=L,y}=0 \tag{14}$$

$$\left(\frac{\partial \omega}{\partial x}\right)_{y,z=0}+\left(\frac{\partial \omega}{\partial y}\right)_{x,z=0}=0 \tag{15}$$

$$\left(\frac{\partial \omega}{\partial x}\right)_{z,y=0}+\left(\frac{\partial \omega}{\partial z}\right)_{x,y=0}=0 \tag{16}$$

- at the material-air interface (y = 0 and y = l), the continuity of liquid and vapor flows satisfies the following expressions:

$$\begin{bmatrix} \dot{m}_l+\dot{m}_v \\ \dot{m}-L_v\dot{m}_l \end{bmatrix}=\begin{bmatrix} \beta(p_v^{sat}(T_{ext})\omega_{ext}-p_v^{sat}(T_{\text{int}})\omega_{\text{int}} \\ \alpha(T_{ext}-T_{\text{int}}) \end{bmatrix} \tag{17}$$

In this expression, T_{ext} is the outdoor ambient temperature and the outdoor humidity rate, which varies over time depending on the simulation period.

3.numerical resolution method

The model was solved using COMSOL Multiphysics® numerical calculation software.For numerical simulation, the system is subdivided into two sub-domains (BTC block and air). We chose the “normal” mesh type for the complete 3D geometry. A triangularmeshwithseveralelementswaschosen. The meshschematic for the wall studied is shown in Figure 3.Since the study regime is unsteady, the time duration is set at 7 hours as the maximum exposure time for the wall of an open-air building.The time step is set to one (01) hour and the relative tolerance to 0.001 for all parameters.With reference to the coupled equations developed above, we have adapted them to the COMSOL Partial Derivative Equation (PDE) by:

$$e_a\frac{\partial^2 u}{\partial t^2}+d_a\frac{\partial u}{\partial t}+\nabla(-c\nabla u-\alpha u+\gamma)+\beta\nabla u+\alpha' u=f \tag{18}$$

where u is the coupled state variable (temperature T and humidity).Some coefficients have been chosen to be zero, given the form of the PDE to be solved.The final form adopted is that given by equation (19). To solve the problem in COMSOL, equation (6) was written in its matrix form:

$$d_a\begin{bmatrix} \dfrac{\partial T}{\partial t} \\ \dfrac{\partial \omega}{\partial t} \end{bmatrix}=\nabla.\left(C\nabla\begin{bmatrix} T \\ \omega \end{bmatrix}\right)+\beta.\nabla\begin{bmatrix} T \\ \omega \end{bmatrix} \tag{19}$$

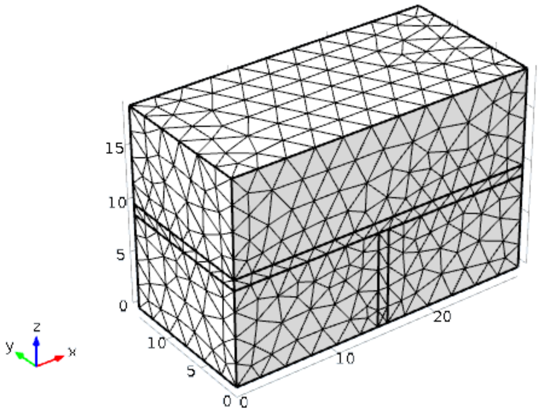

Figure 3: Mesh schematic

The discretization scheme is of the Lagrange-linear type (finite element method).The convergence criterion is of the order of 10^{-3} for all equations.

4.Results and discussions

Figures 4.a, 4.b and 4.c show temperature profiles for wall thicknesses of 15 cm, 50 cm and 100 cm respectively, as a function of exposure time.These profiles represent the temperature evolution in the bricks from x = 0 up to thickness e, at particular instants.For the different thicknesses considered, the temperature evolution goes from the stressed wall to the unstressed one.We note that the temperature gradually decreases along the wall and stabilizes at around 40 cm thickness over the entire 6-hour exposure period.Mnasri (2017) made a similar observation in his work on composite materials in France.

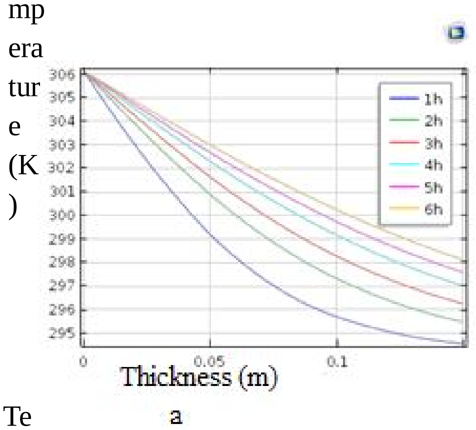

a

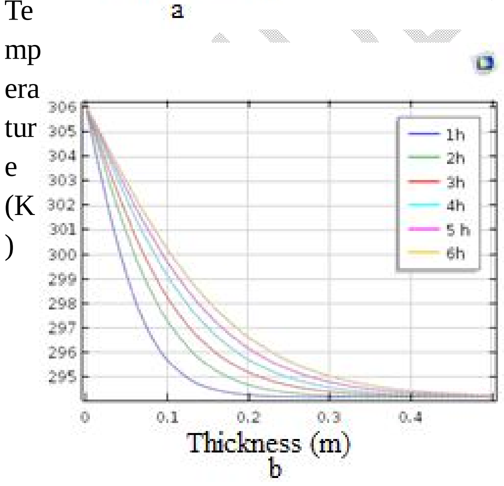

b

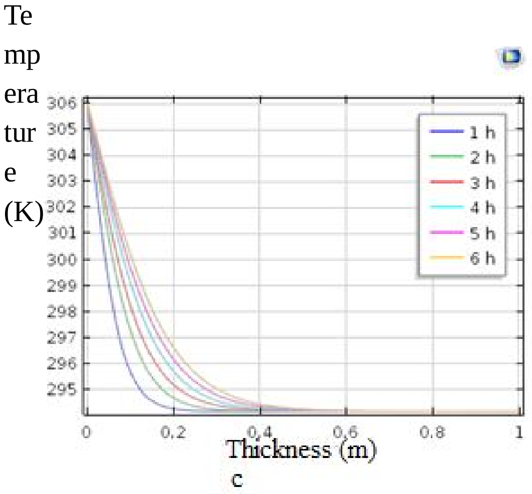

c

Figure 4: Temperature profiles through the wall as a function of thickness.

Mo ist ure co nte nt (.)

Figures 5.a, 5.b and 5.c show water content profiles for wall thicknesses of 15 cm, 50 cm and 100 cm respectively, as a function of exposure time.Moisture content was recorded from the stressed to the unstressed wall.We note that the moisture content gradually decreases from 0.21 to 0.11 along the wall and stabilizes at 0.10 for a thickness of around 40 cm for the entire duration of 6 h of exposure.

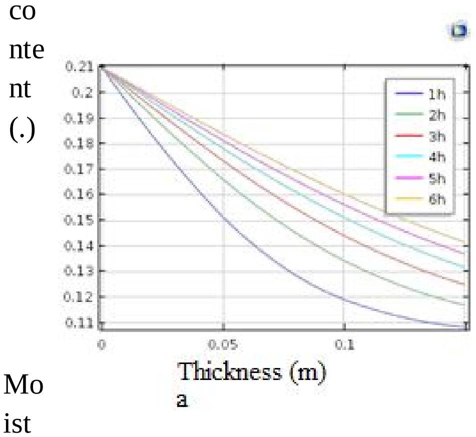

a

Mo ist ure co nte nt (.)

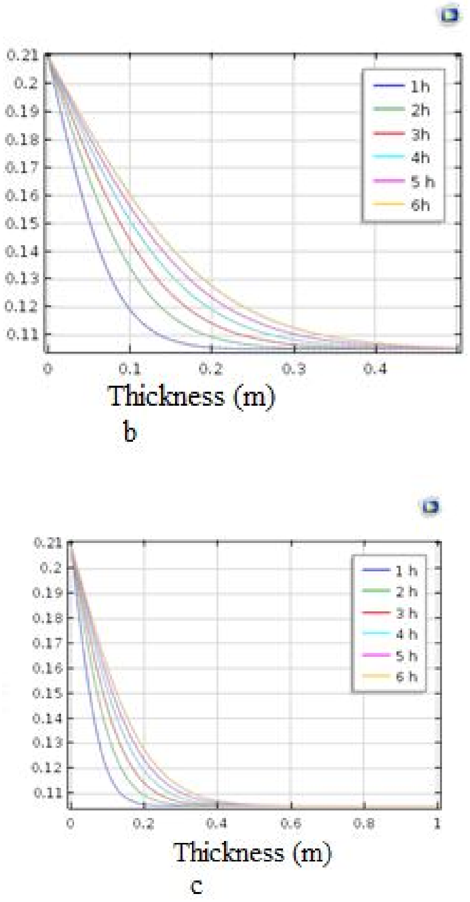

Figure 5: Moisture content versus thickness profiles across the wall

Figure 6 shows the temperature profile as a function of thickness.We can see that as thickness increases, the wall takes longer to react.In other words, it heats up slowly.For a block thickness of 15 cm, the reaction time is approximately one (01) hour.For a thickness of 50 cm, this is around ten (10) hours, whereas a building wall cannot be exposed for more than 6 hours in our tropics.

As for the maximum thickness of 100 cm, the block remains virtually unaffected by thermal stress.To guarantee thermal inertia with blocks of the same type, you need a thickness of between 15 cm and 50 cm.According to (Bekkouche et al. 2010), the thickness thermogram with the smallest amplitude provides the best comfort compromise.If our BTC blocks are to be used in the future, and thermal comfort in the room is to be guaranteed, it is imperative to change the installation technique.For this purpose, we recommend a “boutisse” block installation technique (CSTB-2588 2012).

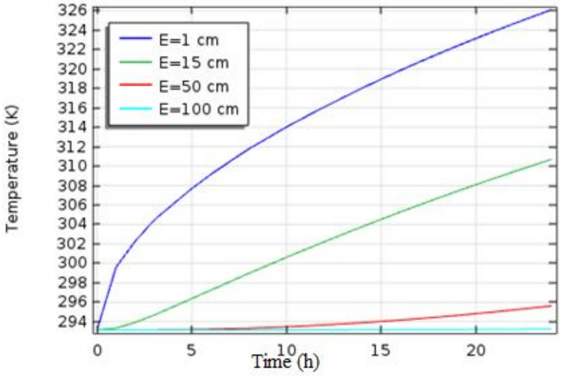

Figure 6: Temperature profile for different thicknesses

Conclusion

The present work studies numerically the coupled heat and mass transport within a wall made of BTC.The model considers temperature and moisture content as variables for heat and mass transfer respectively.The model was successfully calibrated by solving a coupled PDE (partial differential equation) in 3D under COMSOL.The results of this work illustrate the thermal and mass exchanges that take place in a wall made with BTC blocks. This study shows that:

- the response of a BTC wall to thermo-hydric stress depends on its thickness.

- the thicker the BTC wall, the more it dampens temperature and water content. The optimum wall thickness for a BTC building is around 40 cm.

References

1.Institut de la Francophonie pour le Développement Durable, numéro 94 2ème et 3ème trimestre 2013, énergies renouvelables : productions distribuées et communautaire

2.Etienne M., David Y.K.T, Joseph B., Jean K., *Hygrothermal behavior of two buildings constructed in cement bricks and cut laterite blocks,* International conference on Energy, Environment and Economics, 11-13 December 2017

3. Emmanuel O., Ousmane C., Kossi B. I., Ouamnoaga A. G. K., Abdoulaye O., Florent P. K. ,Diendonné J. B., Designing an Energy-Efficient Building in a Context of Helping Self-Build, American Journal of Energy Engineering 2018; 6(3): 29-37 http://www.sciencepublishinggroup.com/j/ajee

4. Lamyaa L., Laurent U., Sylvie Y., Jean-Emmanuel A., Pascal M., *Simulation of the Hygro-Thermo-Mechanical Behavior of Earth Brick Walls in Their Environment,* Buildings 2023, 13, 3061. https://doi.org/10.3390/buildings13123061

5. Lamyaa Laou, Laurent Ulmet, Sylvie Yotte, Jean-Emmanuel Aubert, and Pascal Maillard, *simulation of the Hygro-Thermo-Mechanical Behavior of Earth Brick Walls in Their Environment,*Buildings 2023, 13, 3061. https://doi.org/10.3390/buildings13123061

6. Meriem S., Amel S. C., Ezeddine S., Belkacem Z. *Hygrothermal Behavior of Earth-Based Materials: Experimental and Numerical Analysis,* MATEC Web of Conferences 330, 01030 (2020)

7. Madeleine N., Donatien N., Pierre M. and Cyrille F. T., *Modeling of Coupled Heat and Mass Transfers in a Stabilized Earthen Building Envelope with Thatched Fibers, Fibers2018, 6, 75; doi:10.3390/fib6040075 www.mdpi.com/journal/fibers*

8. Mohamed S., Alexandre G.,Marie D., Ameur E. A. H., Rafik B. *A Review on Numerical Modeling of the Hygrothermal Behavior of Building Envelopes Incorporating Phase Change Materials,* Buildings 2023, 13, 3086. https://doi.org/10.3390/buildings13123086

9.Luikov, A.V. 1975. « Systems of differential equations of heat and mass transfer in capillary-porous bodies ». *International Journal of Heat Mass Transfer* 18: 1–14.

10.Philip. J. R., DE Vries. D. A.*Moisture Movement in Porous Materials under Temperature Gradients,* Transaction American Geophysical Union, Vol. 38, N°2, April 1957

11.Crausse P., G. Bacon, et S. Bories. 1981. « *Etude fondamentale des transferts couples chaleur-masse en milieu poreux* ». *International Journal of Heat and Mass Transfer* 24 (6): 991–1004. https://doi.org/10.1016/0017-9310(81)90130-7.

12**.** K. ABAHRI, R. BELARBI, A. TRABELSI, *Contribution to analytical and numerical study of combined heat and moisture transfers in porous building materials,*Building and Environment 46 (2011) 1354-1360.,

13.J. E. AUBERT**,** *Caractérisation des briques de terre crue de Midi-Pyrénées*, Rapport final du projet TERCRUSO, avril 2013.

14.Kabre Sayouba, François Ouedraogo, Bétaboalé Naon, et Adamah Messan. 2019. « *Évaluationdes propriétés thermo-hydro-mécaniques des briques en terre compressée (BTC) issues de la carrière de Matourkou , au Burkina Faso* » 15 (3): 12–22. *Afrique Science*.

15. Youchao Zhang, Shuangli Jiang, Dengzhou Quan, Kun Fang, Bo Wang and Zhiming Ma, *Properties of Sustainable Earth Construction Materials: A State-of-the-Art Review, MDPI,* Sustainability 2024, 16, 670. https://doi.org/10.3390/su16020670